Published OnlineFirst April 6, 2010; DOI: 10.1158/1535-7163.MCT-09-1220

Research Article

Molecular Cancer Therapeutics

Nutlin-3a Induces Cytoskeletal Rearrangement and Inhibits the Migration and Invasion Capacity of p53 Wild-Type Cancer Cells

Diarmuid M. Moran and Carl G. Maki

Abstract

MDM2 is an E3 ubiquitin ligase that binds and ubiquitinates the tumor suppressor protein p53, leading to its proteasomal degradation. Nutlin-3a (Nutlin) is a preclinical drug that binds MDM2 and prevents the interaction between MDM2 and p53, leading to p53 stabilization and activation of p53 signaling events. Previous studies have reported that Nutlin promotes growth arrest and/or apoptosis in cancer cells that express wild-type p53. In the current study, Nutlin treatment caused a cytoskeletal rearrangement in p53 wild-type human cancer cells from multiple etiologies. Specifically, Nutlin decreased actin stress fibers and reduced the size and number of focal adhesions in treated cells. This process was dependent on p53 expression but was independent of p21 expression and growth arrest. Consistent with this, Nutlin-treated cells failed to form filamentous actin–based motility structures (lamellipodia) and displayed significantly decreased directional persistence in response to migratory cues. Finally, chemotactic assays showed a p53-dependent/p21-independent decrease in migratory and invasive capacity of Nutlin-treated cells. Taken together, these findings reveal that Nutlin treatment can inhibit the migration and invasion capacity of p53 wild-type cells, adding to the potential therapeutic benefit of Nutlin and other small molecule MDM2 inhibitors. *Mol Cancer Ther; 9(4); 895–905. ©2010 AACR.*

Introduction

The tumor suppressor p53 is one of the most commonly mutated proteins in human cancers. Wild-type p53 is a transcription factor that induces cell cycle arrest, apoptosis, or senescence in response to internal or external stresses that might otherwise predispose normal cells to cancer (1, 2). When p53 is mutated, it is unable to inhibit growth in response to these stresses, leading to tumor development. Approximately 50% of human tumors express wild-type p53; however, p53 function is generally compromised in these cancers due to abnormalities in the way in which p53 is regulated or defects in the p53 signaling pathway (3). MDM2 is the major negative regulator of p53, and *mdm2* gene amplification is a common abnormality observed in cancers that retain wild-type p53 (4). MDM2 is an E3 ligase that binds to and ubiquitinates p53, leading to its proteasomal degradation (5, 6). p53 and MDM2 form an autoregulatory feedback loop in which p53 transcriptionally activates the expression of MDM2, and MDM2 stimulates the degradation of p53, thereby controlling the levels of both proteins. Nutlin-3a (Nutlin) is a *cis*-imidazoline compound that specifically binds MDM2 and prevents the interaction between MDM2 and p53 (7). Therefore, in the presence of Nutlin, p53 does not undergo proteasomal degradation and p53 protein accumulates in the cell. p53 can then inhibit proliferation and/or cause cell death (7, 8). Nutlin treatment has been shown to inhibit the growth of human tumors that express wild-type p53 in nude mice xenograft models (7).

Metastasis from a tumor tissue of origin to distant sites constitutes the most life-threatening aspect of cancer (9). To metastasize, cells must become motile and invasive to surrounding tissues. The actin cytoskeleton is remodeled during cell movement, primarily through activity of the Rho family of small GTPases (RhoA, Rac1, and Cdc42; ref. 10). In response to migratory cues, cells initially become polarized, forming a leading edge in the direction of movement. Active Cdc42 localizes at the leading edge of the cell and induces localized *de novo* polymerization of actin to form filipodia (spike-like structures of actin) through regulation of the activity of the WASP (Wiskott-Aldrich syndrome protein) protein

Authors' Affiliation: Department of Radiation and Cellular Oncology, University of Chicago, Chicago, Illinois

Note: Supplementary material for this article is available at Molecular Cancer Therapeutics Online (http://mct.aacrjournals.org/).

Current address for D.M. Moran: Lurie Comprehensive Cancer Center, Northwestern University, Department of Hematology/Oncology, 303 East Superior Street, Room 6220, Chicago, IL 60610.

Current address for C.G. Maki: Rush University Medical Center, Department of Anatomy and Cell Biology, 1653 West Congress Parkway, Jelke 1306, Chicago, IL 60612.

Corresponding Author: Carl Maki, Rush University Medical Center, Department of Anatomy and Cell Biology, 1653 West Congress Parkway, Jelke 1306, Chicago, IL 60612. Phone: 312-563-3632; Fax: 312-942-5744. E-mail: Carl_Maki@rush.edu

doi: 10.1158/1535-7163.MCT-09-1220

Published OnlineFirst April 6, 2010; DOI: 10.1158/1535-7163.MCT-09-1220

complex (11, 12). Active RAC1 at the leading edge of cells stimulates the formation of lamellipodia (flat sheet-like structures of actin) through the regulation of WAVE (WASP family verprolin-homolous protein) complexes. These multiprotein complexes are recruited to the membrane at the cell leading edge and, once active, associate with and stimulate the activity of the actin nucleating proteins actin-related proteins 2 and 3, leading to actin polymerization. Integrin-dependent focal adhesions form between these newly formed actin-rich protrusions (lamellipodia) and the ECM (11, 12). The cell body follows the leading edge while retracting the lagging tail. Rho A regulates cell contractility through formation of acto-myosin stress fibers and focal adhesions. RhoA has been shown to be required for retraction of the lagging tail of the cell during cell movement (11). An amoeboid form of cancer cell movement has also been described (13). Amoeboid movement leads to faster migration rates and is controlled by the action of RhoA signaling through its effector ROCK. In this form of movement, RhoA-ROCK promotes remodeling of cortical actin that generates propulsion through ECM.

Recent reports support a relationship between p53 and the cytoskeleton. p53 overexpression decreased actin stress fiber levels and focal adhesions in p53-null mouse fibroblasts (14). Other studies showed reduced Cdc42-dependent filipodia formation in mouse embryo fibroblasts (MEF) overexpressing p53, which prevented cell polarization and inhibited cell spreading (15). Similarly, deletion of p53 in MEFs (p53 null) led to cytoskeletal rearrangement and increased cell motility and invasion associated with increased Rac1 activity (16, 17). More recently, deletion of p53 in MEFs was reported to promote RhoA-ROCK–dependent amoeboid cell movement in three-dimensional matrices (18). Taken together, these data suggest a role for p53 in the control of cell migration/invasion through its effects on the actin cytoskeleton. Results from the current study show that Nutlin-treated cancer cells display p53-dependent rearrangement of the actin cytoskeleton, fail to form actin-based motility structures in response to migratory cues, and have diminished chemotactic migration and invasion capacity. These results indicate that clinical use of Nutlin may inhibit directional migration and have antimetastatic potential against p53 wild-type cancers in addition to its already established antiproliferative effects.

Materials and Methods

Cells

HT1080, U2OS, SAOS, and A549 cells were obtained from American Type Culture Collection and had been passaged for <6 mo. Cells were grown in DMEM supplemented with 100 units per mL penicillin, 100 μg/mL streptomycin, and 10% fetal bovine serum (FBS). Cells were plated 24 h before treatment with Nutlin. Nutlin was purchased as a racemic mix of Nutlin-3a (active enantiomer) and Nutlin-3b (inactive enantiomer) from Sigma-Aldrich. All stated doses of Nutlin refer to the active Nutlin-3a enantiomer. Where indicated, plates/coverslips were coated with rat tail collagen I, mouse collagen IV, or human fibronectin (5 $\mu g/cm^2$, BD Biosciences) as the manufacturer describes before plating cells.

Immunoblots

Cells were lysed in 50 mmol/L Tris (pH 7.5), 150 mmol/L NaCl, 0.5% Nonidet P-40, phenylmethylsulfonyl fluoride, and leupeptin. Lysates resolved by SDS-PAGE were transferred to nitrocellulose, blocked with 5% milk, incubated in primary antibody overnight and secondary antibody for 1 h, and visualized by chemiluminescence. Primary antibodies were p53 (ab-2; Calbiochem), actin, tubulin, MDM2 (SMP14), and p21 (H164; Santa Cruz). Densitometry was done using NIH image J software, and values were corrected for actin/tubulin loading control. Significance was determined using Student's *t*-test ($P < 0.05$).

Immunofluorescence/cytoskeletal staining

Immunofluorescence cytoskeletal staining was done using an actin cytoskeleton/focal adhesion staining kit (Millipore). Briefly, cells were fixed on cover glass with 4% paraformaldehyde, blocked in 1% bovine serum albumin and 0.1% Triton X-100 and incubated with primary antibodies (1:100 dilution) for 1.5 h. Cells were next incubated with TRITC-conjugated phalloidin (Millipore; 1:100 dilution) and Alexa 488–conjugated secondary antibody (1:2,000 dilution; Invitrogen) and/or Cy5-conjugated secondary antibody (1:2,000; Jackson Immunoresearch) for 1 h. Primary antibodies were anti-vinculin (Millipore), anti-p21 (H-164), and anti-p53 (FL-393; Santa Cruz). To visualize lamellipodia formation, cells were grown to confluency on collagen-coated coverslips, and cell monolayer was wounded 2 h before fixation. Samples were visualized and imaged using a Zeiss Axiovert 200 M fluorescence microscope. Cy5 staining was pseudocolored orange in all images. Image analysis was done using NIH Image J analysis software.

Cell cycle analysis

Cells were trypsinized and resuspended in PBS (0.1% bovine serum albumin). A total of 1.5×10^6 cells per mL were fixed in ethanol (4°C), resuspended in RNase A (0.7 mg/mL)/propidium iodide (50 mg/mL), and incubated at 37°C. Analysis was done using FACSCanto flow cytometer (BD Biosciences), and data were analyzed using Flowjo software.

siRNA-mediated transient knockdown

p53 RNAi, p21 RNAi, and control RNAi (On-target plus siControl nontargeting pool) were purchased from Dharmacon and transfected according to the manufacturer's guidelines using DharmaFECT I reagent. Treatments were applied 24 h after transfection.

Published OnlineFirst April 6, 2010; DOI: 10.1158/1535-7163.MCT-09-1220

Time lapse microscopy

HT1080 cells were grown to confluency in collagen-coated six-well dishes. Cell monolayer was wounded using a sterile micropipette tip, and cells at multiple points along the wound edge were imaged every 5 min over a 4-h period using a Zeiss Axiovert 100 microscope. Cells were maintained at 5% CO_2 and 37°C during the course of these experiments. Cell track analysis of individual cells, determination of velocity, and directional persistence were done using Metamorph version 7.6 image analysis software (50 cells per wound edge).

Chemotactic migration assay

Chemotactic migration was studied using BD Biosciences 24-well uncoated migration chambers (8.0-μm pore size; BD Biosciences) as follows. Approximately 2.5×10^4 (1.25×10^4 for HT1080) untreated or Nutlin-pretreated (8 μmol/L, 24 h) cells were seeded in the upper chambers of the plate in triplicate in 500 μL serum-free DMEM (±Nutlin). DMEM with 10% FBS (±Nutlin) was added to the lower chamber as a chemoattractant. After 24 h of incubation at 37°C with 5% CO_2, cells remaining on the upper membrane surface were removed with a cotton swab. Cells on the lower surface of the membrane were stained with crystal violet and fixed in methanol. The invasive cells on the lower surface of membrane were counted using a microscope. Each experiment was repeated thrice. To control for effects on cell proliferation, cells were dislodged from additional intact membranes using trypsin (15 min at 37°C) and vortexing. Total cell number was counted using a hemocytometer.

Matrigel invasion assay

Invasion of cells through Matrigel-coated membranes was determined using 24-well BD invasion chambers (8.0-μm pore size; BD Biosciences) in accordance with the manufacturer's instructions with the following modifications. Briefly, cells were trypsinized, and 2.5×10^4 (1.25×10^4 for HT1080) untreated or Nutlin-pretreated (8 μmol/L, 24 h) cells were placed into the upper compartment of the invasion plates in triplicate in 500 μL serum-free DMEM (±Nutlin). The lower compartment was filled with 750 μL of 10% FBS DMEM (±Nutlin). After 40 h of incubation at 37°C with 5% CO_2, cells remaining on the upper membrane surface were removed with a cotton swab. Cells on the lower surface of the membrane were stained with crystal violet and fixed in methanol. The invasive cells on the lower surface of membrane were counted using a microscope. Each experiment was repeated thrice. To control for effects on cell proliferation, cells were dislodged from additional intact Matrigel membranes using trypsin (2 h at 37°C) and vortexing. Total cell number was counted using a hemocytometer.

Results

Previous studies describe increased p53 levels and activity in p53 wild-type cancer cells (p53wt) upon treatment with the MDM2 inhibitor Nutlin-3a (Nutlin; refs. 7, 8). We treated human cancer cell lines U2OS (osteosarcoma; p53wt), A549 (lung adenocarcinoma; p53wt), HT1080 (fibrosarcoma; p53wt), and SAOS (osteosarcoma; p53 null) with increasing doses of Nutlin (0–16 μmol/L, 24 h) and monitored the expression of p53, p21, and MDM2 by immunoblotting (data not shown). Nutlin treatment caused a dose-dependent increase in p53 and its downstream targets p21 and MDM2 in p53wt cells. A robust increase in p53 was observed in p53wt cell lines in our study at an 8 μmol/L Nutlin dose (Fig. 1A). As expected, Nutlin did not induce p53, p21, or MDM2 expression in SAOS cells. Next, we analyzed cell cycle profiles in Nutlin-treated cells. DNA content analysis showed that Nutlin treatment of p53wt cell lines (U2OS, A549, and HT1080) caused these cells to arrest with 2N and 4N DNA content, suggestive of G_1-phase and G_2-phase cell cycle arrest. In contrast, the same Nutlin treatment had no obvious effect on the cell cycle profile of p53-null SAOS cells (Fig. 1B). Analysis of sub-G_1 populations in these cells showed no detectable increase in cell death at 24 or 48 hours after Nutlin treatment.

During the course of our studies, we observed a dose-dependent alteration in cellular morphology in Nutlin-treated p53wt cells. Typically, cell structure changed from a well-spread polygonal structure to a more elongated morphology (Supplementary File S1) during Nutlin treatment, becoming apparent at 24 hours and occurring in ~70% of cells at 40 hours after treatment (16 μmol/L Nutlin). Morphologic changes were most apparent at higher Nutlin doses (8–16 μmol/L), coincident with

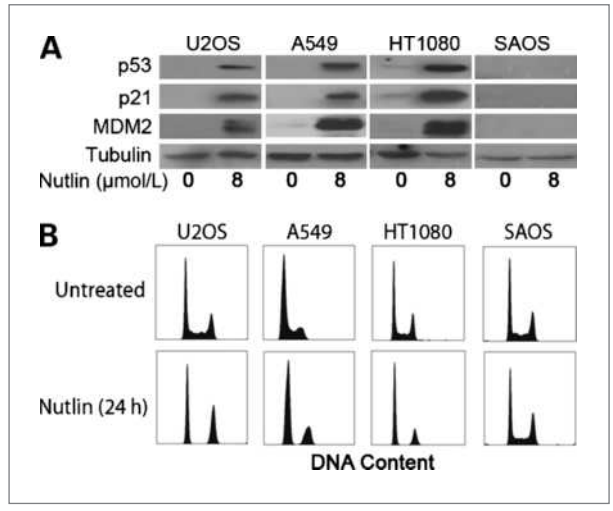

Figure 1. Nutlin increases p53 expression/activity and induces growth arrest in p53wt human cancer cells. A, representative immunoblots from U2OS, A549, HT1080, and SAOS cell lysates collected 24 h after Nutlin treatment (8 μmol/L) probed using antibodies specific against p53, p21, and MDM2. Actin expression was detected as a loading control. B, representative DNA content profiles of untreated and Nutlin-treated (8 μmol/L) U2OS, A549, HT1080, and SAOS cells. Cells were fixed, stained with propidium iodide, and analyzed by flow cytometry for DNA content. DNA profiles are representative of three independent experiments.

Published OnlineFirst April 6, 2010; DOI: 10.1158/1535-7163.MCT-09-1220

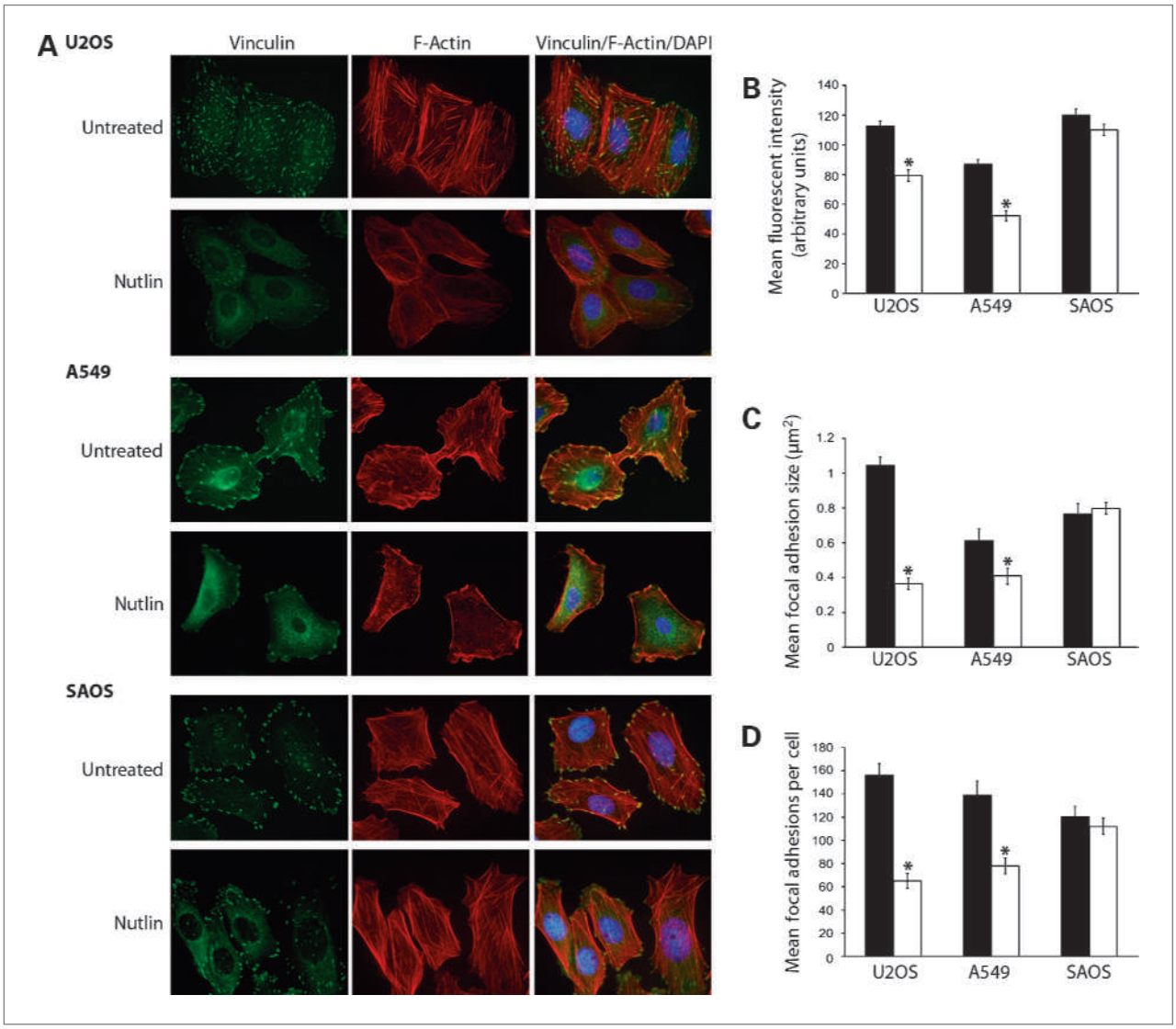

Figure 2. Nutlin decreases F-actin stress fibers and focal adhesion size and number in p53wt human cancer cells. A, representative immunofluorescence images of Nutlin and untreated U2OS, A549, and SAOS cells. Cells seeded on collagen-coated coverslips were treated with Nutlin (8 μmol/L, 40 h) or left untreated and stained for focal adhesions (green) and F-actin stress fibers (red). Nuclei were visualized by 4′,6-diamidino-2-phenylindole (DAPI) staining (blue). Images are representative of three independent experiments, each with 200 cells analyzed per experiment. B, mean fluorescence intensity of rhodamine-conjugated phalloidin staining per cell was determined using image J analysis software in U2OS, A549, and SAOS cells seeded on collagen-coated coverslips with or without Nutlin treatment (8 μmol/L, 40 h). C and D, mean focal adhesion size and number stained with anti-vinculin antibody were determined using image J analysis software in U2OS, A549, and SAOS cells seeded on collagen-coated coverslips with or without Nutlin treatment (8 μmol/L, 40 h). Data are representative of three independent experiments, each with 200 cells analyzed per experiment (*, $P < 0.05$ Nutlin-treated versus untreated).

increased levels of p53. This alteration in morphology was reversible, and cells returned to a spread/polygonal morphology within 8 hours after Nutlin removal (data not shown). These morphologic changes were also observed when Nutlin-treated cells were plated on individual ECM surfaces, including fibronectin, collagen IV, and collagen I (data not shown). Because cellular morphology is controlled by the actin cytoskeleton, we examined cytoskeletal organization of Nutlin-treated p53wt and p53 null cells 40 hours after treatment. Cells were plated on collagen-coated coverslips, treated with Nutlin (8 μmol/L), and stained with rhodamine-conjugated phalloidin to detect filamentous actin (F-actin) and anti-vinculin antibody to detect focal adhesions. Untreated A549 and U2OS cells display numerous large actin stress fibers and large focal adhesions throughout the cell body. Treatment with Nutlin decreased F-actin stress fibers and focal adhesion size and number in A549 and U2OS cells (Fig. 2A). Image analysis showed significantly decreased phalloidin staining intensity in treated versus untreated cells, confirming the decrease

Published OnlineFirst April 6, 2010; DOI: 10.1158/1535-7163.MCT-09-1220

in F-actin expression after treatment (Fig. 2B). In addition, image analysis indicated a decrease in the size and number of focal adhesions with Nutlin treatment (Fig. 2C and D). Nutlin also induced cytoskeletal rearrangement in HT1080 cells (Supplementary File S2). These effects seemed to depend on p53 status, because F-actin expression/cytoskeletal arrangement were not diminished/altered by Nutlin treatment in p53 null SAOS cells, and there was also little to no effect of Nutlin on focal adhesion number or size in these cells (Fig. 2A–D). It is worth noting that Nutlin treatment was also associated with an increase in cytoplasmic (nonadhesion-associated) vinculin staining in all cell types. This, however, does not seem to relate to the decrease in focal adhesion size and number, as it was also apparent in SAOS cells wherein adhesions remain unaffected by Nutlin treatment.

Next we wished to test the dependency of these effects on p53 and the p53 downstream effector, p21. U2OS cells were transfected with siRNA targeting p53 (sip53), p21 (sip21), or a nontargeting siRNA sequence (siCTRL) before treatment with Nutlin (8 μmol/L, 24 hours later). U2OS cells were used for these studies as they showed the most efficient knockdown of p53 and p21 expression compared with other cells. Lysates from Nutlin-treated and untreated cells were collected 40 hours after Nutlin treatment and immunoblotted for p53 and p21 expression. Cells transfected with siCTRL showed increased expression of p53 and p21 with Nutlin treatment (Figs. 3A and 4A). In contrast, sip53-transfected cells did not show a detectable increase in p53 or p21 expression after Nutlin treatment (Fig. 3A), and cells transfected with sip21 showed increased p53 but no increase in p21 (Fig. 4A and C). Cell cycle analysis showed that sip53 (Fig. 3B) and sip21 (Fig. 4B) ablated Nutlin-induced cell cycle arrest in U2OS cells. Untreated and Nutlin-treated sip53-, sip21-, and siCTRL-transfected U2OS cells were next stained for stress fibers/focal adhesions. As expected, cells transfected with control siRNA showed diminished F-actin stress fiber levels, as well as decreased focal adhesion size and number with Nutlin treatment (Fig. 3C). In contrast, sip53-transfected cells retained normal actin stress fiber levels with Nutlin treatment, and the number and size of focal adhesions were unaffected (Fig. 3C). These results confirm that cytoskeletal changes induced by Nutlin treatment are p53 dependent. Interestingly, cells in which p21 was knocked down also displayed decreased F-actin stress fiber levels and a decrease in the number and size of focal adhesions after Nutlin treatment, similar to control cells (Fig. 4D). This indicates that p21-dependent cell cycle arrest is not associated with or required for these cytoskeletal changes.

Reorganization of the actin cytoskeleton is essential for cell migration and invasion (11, 12). We therefore hypothesized that Nutlin might also affect the formation of actin-based motility structures in cancer cells. In a wound assay, cells grown in a confluent monolayer form large

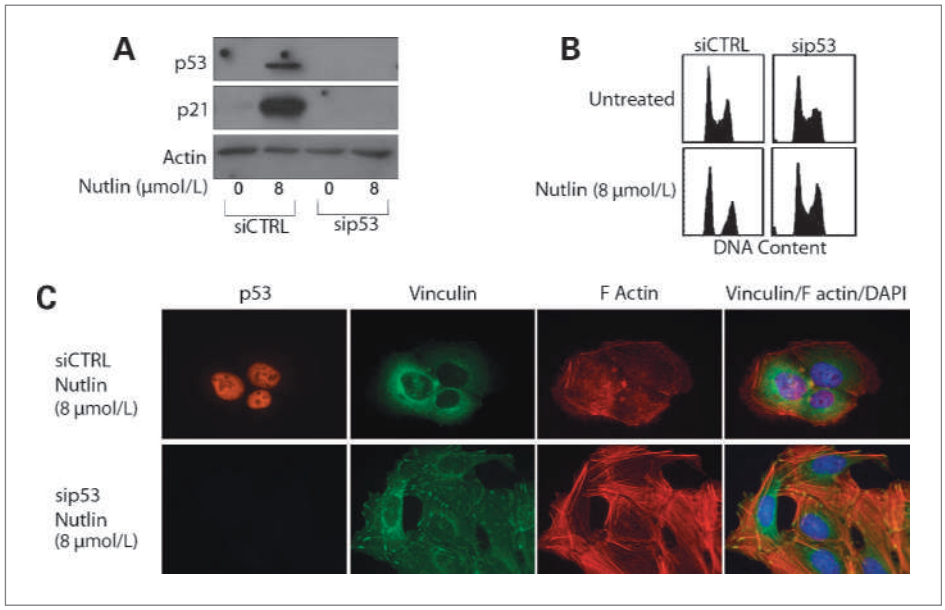

Figure 3. Nutlin-induced cytoskeletal rearrangement is dependent on p53 expression. U2OS cells were transfected with siRNA targeting p53 (sip53) or a nontargeting control sequence (siCTRL). Cells were treated with Nutlin 24 h later or left untreated. A, representative immunoblots from siCTRL and sip53-transfected U2OS cell lysates collected 24 h after Nutlin treatment (8 μmol/L) probed using antibodies specific against p53 and p21. Actin was detected as a loading control. B, representative DNA content profiles of untreated and Nutlin-treated (8 μmol/L) sip53 and siCTRL-transfected U2OS. Cells were fixed, stained with propidium iodide, and analyzed by flow cytometry for DNA content. DNA profiles are representative of three independent experiments. C, representative fluorescence images of Nutlin and untreated sip53 and siCTRL U2OS cells. Cells seeded on collagen-coated coverslips were treated with Nutlin (8 μmol/L, 40 h) or left untreated and stained for focal adhesions (green), p53 (orange), and F-actin stress fibers (red). Nuclei were visualized by DAPI staining (blue). Images are representative of three independent experiments, each with 200 cells analyzed per experiment.

Published OnlineFirst April 6, 2010; DOI: 10.1158/1535-7163.MCT-09-1220

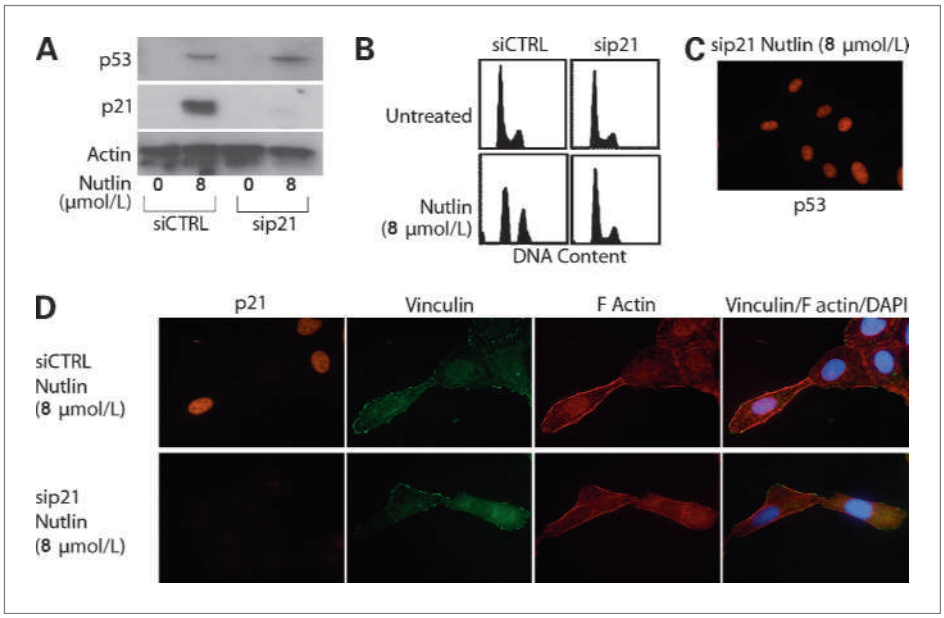

Figure 4. Nutlin-induced cytoskeletal rearrangement is not dependent on p21 expression/growth arrest. U2OS cells were transfected with siRNA targeting p21 (sip21) or a nontargeting control sequence (siCTRL). Cells were treated with Nutlin 24 h later or left untreated. A, representative immunoblots from siCTRL and sip21-transfected U2OS cell lysates collected 24 h after Nutlin treatment (8 μmol/L) probed using antibodies specific against p53 and p21. Actin expression was detected as a loading control. B, representative DNA content profiles of untreated and Nutlin-treated (8 μmol/L) sip21 and siCTRL-transfected U2OS. Cells were fixed, stained with propidium iodide, and analyzed by flow cytometry for DNA content. DNA profiles are representative of three independent experiments. C, representative fluorescence image of Nutlin-treated (8 μmol/L) sip21-transfected U2OS cells. Cells seeded on collagen-coated coverslips were treated with Nutlin (8 μmol/L, 40 h) and stained with an antibody specific against p53 (orange). D, representative fluorescence images of Nutlin and untreated sip21 and siCTRL U2OS cells. Cells seeded on collagen-coated coverslips were treated with Nutlin 8 μmol/L, 40 h) and stained for focal adhesions (green), p21 (orange), and F-actin stress fibers (red). Nuclei were visualized by DAPI staining (blue). Images are representative of three independent experiments, each with 200 cells analyzed per experiment.

sheets of actin (lamellipodia) and strong focal adhesions at the leading edge of the cell as they migrate into the wound (19). To investigate the effect of Nutlin on this process, we wounded a confluent monolayer of Nutlin-treated or untreated U2OS (mildly invasive), SAOS (mildly invasive), and HT1080 (highly invasive) cells on collagen-coated coverslips using a sterile micropipette tip. Two hours after wounding, cells were stained for stress fibers/focal adhesions, and the percentages of wound-edge cells displaying lamellipodia were evaluated. Untreated 2OS, SAOS, and HT1080 cells formed large F-actin–rich lamellipodia at the leading edge of wounded cells (Fig. 5A and B). Nutlin treatment (4 and 8 μmol/L) significantly decreased the percentage of cells displaying lamellipodia in HT1080 and U2OS cells but had no effect on lamellipodia formation in SAOS cells (Fig. 5B). To investigate the dependency of this effect on p53 or p21 expression, Nutlin-treated or untreated U2OS cells transfected with sip53 or sip21 were wounded in a similar assay. Lamellipodia formation was lost in Nutlin-treated siCTRL and sip21 cells; however, lamellipodia formation in sip53-transfected cells remained unaffected by Nutlin treatment (Fig. 5C and D).

Next we analyzed the effects of Nutlin on cancer cell motility. Highly motile HT1080 cells were grown to confluence on collagen-coated plates and wounded using a sterile micropipette tip. Untreated or Nutlin-treated (8 μmol/L, 40 h) cells were monitored using time lapse microscopy for 4 hours after wounding. Untreated cells formed large lamellipodia at the leading edge within 5 minutes after wounding and continued to move unidirectionally into the wound throughout the 4-hour assay (Fig. 6A). In contrast, Nutlin-treated cells formed narrow protrusions and seemed to move randomly rather than in a directional manner. Some Nutlin-treated cells were observed to lose and regain adhesion to the matrix within the 4-hour visualization period (Fig. 6). Migration track analysis of cells that remained attached to the plate (Fig. 6B) showed that Nutlin-treated and untreated cells could move with similar velocities (Fig. 6C); however, Nutlin significantly decreased directional persistence in treated cells (Fig. 6D). In summary, Nutlin treatment did not inhibit the overall motility of HT1080 cells but did inhibit their ability to move in a persistent, directional manner. This lack of directional movement was correlated with altered cytoskeleton in Nutlin-treated cells and decreased formation of actin-rich motility structures (lamellipodia). HT1080 cells are a rapidly migrating cell type and are particularly suitable for this form of directional motility assay, having the ability to close the wound at ~5 to 6 hours after wounding. The slower-moving U2OS cell is less suitable for this type of assay

Published OnlineFirst April 6, 2010; DOI: 10.1158/1535-7163.MCT-09-1220

(wound closure in 24–28 hours); however, we did perform live cell image analysis on untreated and Nutlin-treated U20S cells seeded sparsely (10–20% confluency) in collagen-coated plates (data not shown). Similar to HT1080 cells, Nutlin-treated U2OS cells displayed multiple narrow protrusions and more frequent oscillations when compared with untreated cells. The slow-moving nature of this cell made it unsuitable for image track analysis.

Finally, we examined the effect of Nutlin on chemotactic cancer cell migration and invasion. Nutlin-treated and

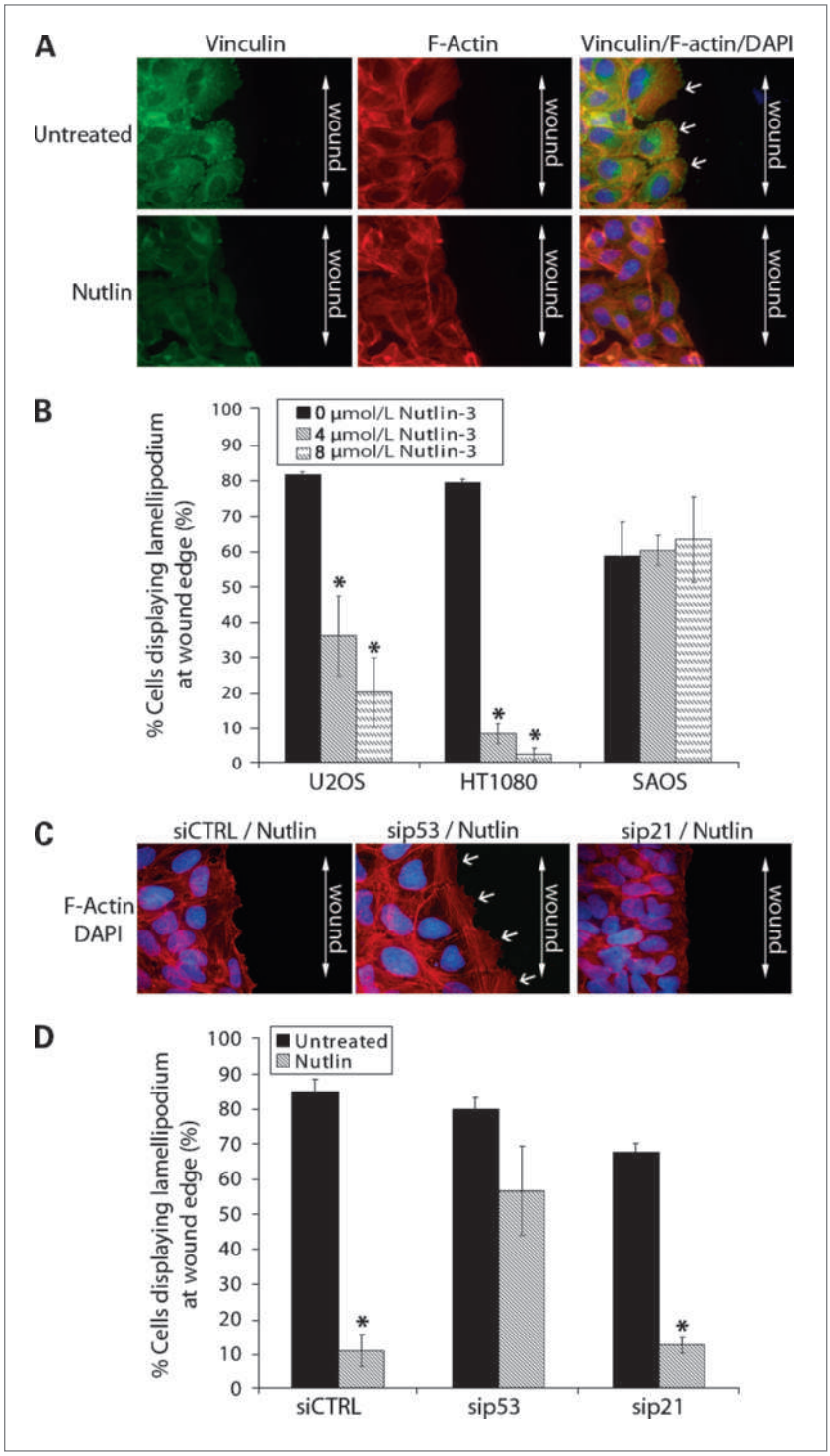

Figure 5. Nutlin decreases lamellipodia formation in wound edge cells in a p53-dependent/p21-independent manner in human cancer cells. A, confluent U2OS, HT1080, and SAOS cells seeded on collagen-coated coverslips were treated with Nutlin (4 μmol/L/8 μmol/L, 40 h) or left untreated. Cells were scratched using a sterile micropipette tip and fixed 2 h later. Representative fluorescence images of Nutlin-treated and untreated U2OS wound edge cells. Cells were stained for focal adhesions (green) and F-actin stress fibers (red). Nuclei were visualized by DAPI staining (blue). Lamellipodia were identified as flat sheets of F-actin (white arrows) at cell leading edges. Images are representative of three independent experiments, each with 200 cells analyzed per experiment. B, percentage of wound edge cells displaying lamellipodia was evaluated and expressed as a percentage of untreated control cells (*, $P < 0.05$ Nutlin-treated versus untreated). C, U2OS cells were transfected with siRNA targeting p21 (sip21), p53 (sip53), or a nontargeting control sequence (siCTRL). Cells were treated with Nutlin (8 μmol/L) 24 h later or left untreated. After 40 h, cells were scratched using a sterile micropipette tip and fixed 2 h later. Cells were stained for F-actin stress fibers (red). Nuclei were visualized by DAPI staining (blue). Lamellipodia was identified as flat sheets of F-actin (white arrows) at cell leading edges. Images are representative of three independent experiments, each with 200 cells analyzed per experiment. D, percentage of siRNA-transfected wound edge cells displaying lamellipodia were evaluated and expressed as a percentage of untreated control cells (*, $P < 0.05$ Nutlin-treated versus untreated).

Published OnlineFirst April 6, 2010; DOI: 10.1158/1535-7163.MCT-09-1220

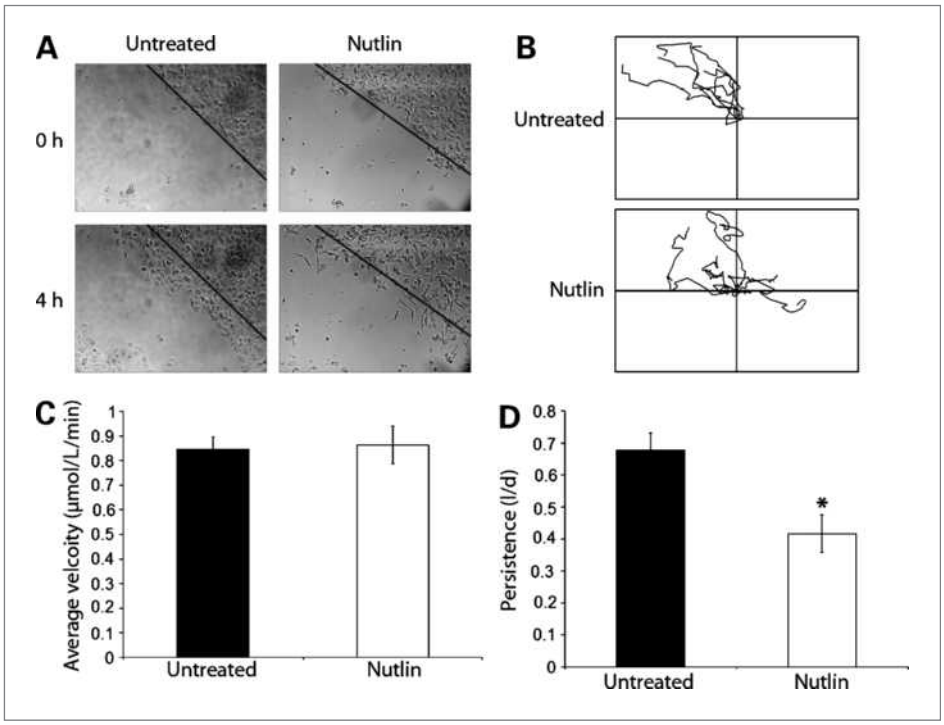

Figure 6. Nutlin decreases directional persistence in HT1080 cells. Confluent HT1080 cells seeded on collagen-coated plates were treated with Nutlin (8 μmol/L, 40 h) or left untreated. Cells were scratched using a sterile micropipette tip and imaged on a time lapse microscope at 5-min intervals over a period of 4 h. A, representative images of Nutlin-treated and untreated HT1080 cells at a wound edge at 0 and 4 h after scratching. Dotted line represents wound edge immediately after wounding (0 h). Images are representative of three independent experiments. B, representative plots of individual Nutlin-treated and untreated HT1080 cell tracks prepared from time lapse microscopy images using Metamorph analysis software. Data are representative of 50 cells per wound edge in three independent experiments. C and D, comparison of average velocity and directional persistence in Nutlin-treated versus untreated HT1080 cells calculated from time lapse microscopy images using Metamorph analysis software. Data are representative of 50 cells per wound edge in three independent experiments (*, $P < 0.05$ Nutlin-treated versus untreated).

untreated U2OS, HT1080, and SAOS cells were initially analyzed for migration and invasion in uncoated boyden chamber or Matrigel-coated invasion chamber assays, respectively. Total cell numbers were also evaluated to control for Nutlin's effect on cell proliferation. Nutlin treatment significantly decreased both migration and invasion of U2OS and HT1080 cells (Fig. 7A and B). Surprisingly, SAOS cell migration and invasion were consistently enhanced by Nutlin treatment in these assays. Similar migration and invasion assays were done in U2OS cells transfected with sip53, sip21, or control siRNA. Nutlin treatment significantly inhibited migration and invasion of U2OS cells transfected with either sip21 or control siRNA (Fig. 7C and D). However, Nutlin did not inhibit migration or invasion of cells transfected with sip53. Thus, Nutlin treatment inhibited the migration and invasion capability of cancer cells in a p53-dependent but p21-independent manner.

Discussion

Nutlin is a small molecule MDM2 antagonist and activator of p53. Results from this study show that Nutlin causes a p53-dependent, but p21-independent, decrease in the level of F-actin stress fibers as well as the number and size of focal adhesions. Consistent with this, Nutlin-treated cells failed to form F-actin–based motility structures (lamellipodia) and displayed significantly decreased directional persistence in response to migratory cues. Finally, chemotactic assays showed a p53-dependent decrease in the migratory and invasive capacity of Nutlin-treated cells. Taken together, these data reveal a previously undescribed cellular response to Nutlin treatment that will likely contribute to its therapeutic and antitumor potential.

The nongenotoxic activation of p53 in p53wt cancer cells represents a promising therapeutic strategy. Previous studies have shown that Nutlin effectively growth arrests p53wt cancer cells in G_1 and G_2 phases, induces senescence, and/or induces apoptosis at low micromolar concentrations in multiple cancer types (7, 8, 20). Moreover, Nutlin administration in nude mice bearing established human cancer xenografts showed effective tumor growth inhibition and tumor shrinkage at nontoxic doses (7). More recently, Sechierro et al. described an inhibitory effect of Nutlin on angiogenesis, which was related at least partially to decreased migratory capacity of treated endothelial cells (21). It has also been shown that Nutlin

Published OnlineFirst April 6, 2010; DOI: 10.1158/1535-7163.MCT-09-1220

can inhibit cancer cell migration and invasion indirectly through repression of stromal-derived factor-1/CXCL12 expression in stromal fibroblasts (22). In the current study, we show for the first time that Nutlin can directly inhibit the migration and invasion capacity of cancer cells that express wild-type p53. Collectively, these results highlight the possibility that Nutlin and similar compounds may act as a combination of antiproliferative, antiangiogenic, and antimetastatic agents, thereby targeting three important events in cancer progression.

In our study, Nutlin altered cell morphology and decreased both actin stress fibers and focal adhesions specifically in p53wt cancer cells. We confirmed the dependency of this phenotype on p53 expression using siRNA targeting p53. Previous studies reported altered morphology and increased focal adhesions in p53-null MEFs (16, 17). Similarly, Alexandrova et al. reported that overexpression of p53 in mouse fibroblasts results in altered cell morphology and reduction in the number and size of actin stress fibers and focal adhesions (14). We considered that Nutlin's effect on the actin cytoskeleton could be an indirect consequence of either cell cycle arrest or apoptosis mediated by p53. However, Nutlin-treated cells in our study exhibit little or no apoptosis as determined by DNA content (sub-G_1) analysis. This allows us to differentiate the cytoskeletal effects of p53 from an apoptotic response. In addition, siRNA knockdown of p21 ablated growth arrest in Nutlin-treated cells but did not prevent the cytoskeletal effects. Based on these findings, we conclude that the cytoskeletal rearrangements induced by Nutlin are independent of either apoptosis or cell cycle arrest mediated by p53.

We identify p53-dependent inhibition of chemotactic/directional migration and invasion in Nutlin-treated cancer cells. We have also discovered abnormalities in the response of Nutlin-treated cells to migratory cues. Specifically, Nutlin-treated cells fail to form lamellipodia in the direction of a wound and display decreased directional

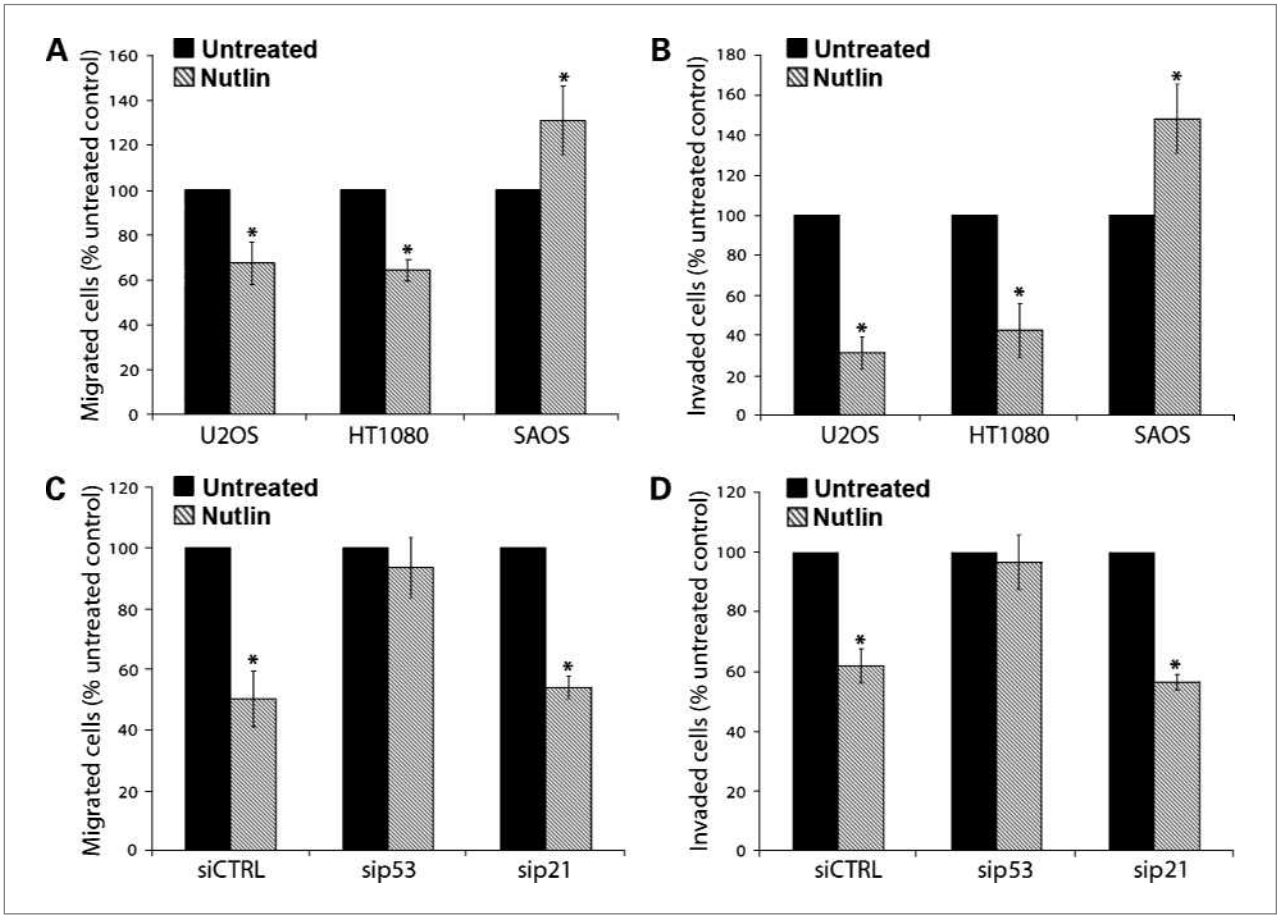

Figure 7. Nutlin decreases cancer cell migration and invasion in a p53-dependent/p21-independent manner. A and B, U2OS, HT1080, and SAOS were treated with Nutlin (8 μmol/L) or left untreated in uncoated (A) or Matrigel-coated (B) boyden chambers. FBS (10%) was added to the lower chamber to act as chemoattractant. After 24 h (migration) or 48 h (invasion), cells were scrubbed from upper surface and migrated/invaded cells were crystal violet stained and counted. Total cell number was calculated by releasing cells on separate membranes and direct counting on a hemocytometer. Data are normalized to total cell number at end of assay. Data are representative of three independent experiments. C and D, U2OS cells were transfected with siRNA targeting p21 (sip21) and p53 (sip53) or a nontargeting control sequence (siCTRL) and were left untreated or treated with Nutlin (8 μmol/L) 24 h later. Migration and invasion assays were done as described above. Data are representative of three independent experiments (*, $P < 0.05$ Nutlin-treated versus untreated).

Published OnlineFirst April 6, 2010; DOI: 10.1158/1535-7163.MCT-09-1220

persistence when compared with untreated cells. It is clear that such abnormalities in cell motility may account, at least in part, for the effect of Nutlin on chemotactic migration and invasion. It is perhaps surprising that Nutlin-treated cells move with similar velocities to untreated cells. However it is worth noting that similar findings have been reported in studies examining the effects of overexpression of tumor suppressors DAPK and Scribble (23, 24). In each case, overexpressing cells migrate with decreased directional persistence and display impaired lamellipodia formation but retain migrational velocity. Taken together, these findings and our study suggest that lamellipodia formation alone is not predictive of migration rate (velocity) in cancer cells. Previous studies have suggested an inhibitory effect of p53 on cell migration and/or invasion (14, 15, 17). In each case, the inhibitory effects of p53 were linked closely with cytoskeletal rearrangement and/or abnormal cell polarization. The mechanism through which p53 mediates its effects on lamellipodia formation and directional persistence in Nutlin-treated cells remains unclear. During cell movement, Rac1 is responsible for the formation of large actin-rich lamellipodial protrusions at the leading edge. In contrast, Cdc42 is responsible for the formation of small, spike-like protrusions (filipodia), and Rho1 functions in the formation of actin stress fibers throughout the cell body, as well as in retraction of the lagging tail. The predominant effect of Nutlin treatment was to diminish F-actin stress fiber levels and inhibit lamellipodia formation at the leading edge, and we therefore monitored Rac1 and RhoA activity in Nutlin-treated HT1080 cells (data not shown). In some but not all experiments, both Rac1 and RhoA activity were inhibited in Nutlin-treated HT1080 cells, suggesting decreased invasion and migration in Nutlin-treated cells might result in part from an inhibition of Rho A and/or Rac1. This would be consistent with previous studies that have reported that high levels of p53 can inhibit RhoA and Rac1 (14, 15, 17).

Taken together, our data uncover novel effects of Nutlin treatment on cancer cell invasion. The most deadly aspect of cancer is its ability to spread or metastasize. During metastasis, primary tumor cells invade the surrounding stroma and migrate toward blood vessels or lymphatics (25, 26). Tumor cells enter blood vessels (intravasation) and are carried by the circulatory system to distant sites where they typically arrest in the capillary bed of a distant organ. The arrested cells extravasate from the circulation system to the organ parenchyma and proliferate to form a secondary tumor. Accumulating evidence suggests that this is not a random process but rather one that is directed by host/tumor signaling. Tumor cells detect and directionally move toward chemoattractant gradients. For example, the chemokine stromal-derived factor-1 can stimulate tumor cell migration away from the primary tumor mass and toward stromal sites in distal organs (27–29). This process is believed to contribute to the metastasis of cancer cells to preferred sites in the body, such as bone, lung, and liver, wherein stromal-derived factor-1 expression is high (30). Similarly, epidermal growth factor and hepatocyte growth factor, which are secreted by cancer-associated fibroblasts and tumor-associated macrophages, have been linked to the guidance of motile/invasive cancer cells (31–33). Directional movement of cancer cells is involved in stromal invasion, intravasation, and extravasation during the metastatic cascade. Interference with directional movement of cancer cells has been shown to decrease metastasis in animal models of cancer (27, 34, 35). Based on our results, Nutlin's inhibitory effects on directional movement and invasion have the possibility to translate into antimetastatic activity. *In vivo* studies to examine the potential antimetastatic effects of Nutlin will be beneficial to establish the relevance of our findings in suitable animal models of cancer.

Disclosure of Potential Conflicts of Interest

No potential conflicts of interest were disclosed.

Grant Support

NIH grant numbers 1RO1CA137598-01A1 and RO1CA108843.
The costs of publication of this article were defrayed in part by the payment of page charges. This article must therefore be hereby marked *advertisement* in accordance with 18 U.S.C. Section 1734 solely to indicate this fact.

Received 12/31/2009; revised 02/09/2010; accepted 02/16/2010; published OnlineFirst 04/06/2010.

References

1. Giono L, Manfredi J. The p53 tumor suppressor participates in multiple cell cycle checkpoints. J Cell Physiol 2006;209:13–20.
2. Harris S, Levine A. The p53 pathway: positive and negative feedback loops. Oncogene 2005;24:2899–908.
3. Hainaut P, Hollstein M. p53 and human cancer: the first ten thousand mutations. Adv Cancer Res 2000;77:81–137.
4. Momand J, Jung D, Wilczynski S, Niland J. The MDM2 gene amplification database. Nucleic Acids Res 1998;26:3453–9.
5. Levav-Cohen Y, Haupt S, Haupt Y. Mdm2 in growth signaling and cancer. Growth Factors 2005;23:183–92.
6. Iwakuma T, Lozano G. MDM2, an introduction. Mol Cancer Res 2003;1:993–1000.
7. Vassilev L, Vu B, Graves B, et al. *In vivo* activation of the p53 pathway by small-molecule antagonists of MDM2. Science 2004;303:844–8.
8. Tovar C, Rosinski J, Filipovic Z, et al. Small-molecule MDM2 antagonists reveal aberrant p53 signaling in cancer: implications for therapy. Proc Natl Acad Sci U S A 2006;103:1888–93.
9. Hanahan D, Weinberg RA. The hallmarks of cancer. Cell 2000;100:57–70.
10. Raftopoulou M, Hall A. Cell migration: Rho GTPases lead the way. Dev Biol 2004;265:23–32.
11. Ridley AJ, Schwartz MA, Burridge K, et al. Cell migration: integrating signals from front to back. Science 2003;302:1704–9.
12. Friedl P, Wolf K. Tumour-cell invasion and migration: diversity and escape mechanisms. Nat Rev Cancer 2003;3:362–74.
13. Sahai E, Marshall C. Differing modes of tumour cell invasion have distinct requirements for Rho/ROCK signalling and extracellular proteolysis. Nat Cell Biol 2003;5:711–9.

Published OnlineFirst April 6, 2010; DOI: 10.1158/1535-7163.MCT-09-1220

14. Alexandrova A, Ivanov A, Chumakov P, Kopnin B, Vasiliev J. Changes in p53 expression in mouse fibroblasts can modify motility and extracellular matrix organization. Oncogene 2000;19:5826–30.
15. Gadéa G, Lapasset L, Gauthier-Rouvière C, Roux P. Regulation of Cdc42-mediated morphological effects: a novel function for p53. EMBO J 2002;21:2373–82.
16. Guo F, Gao Y, Wang L, Zheng Y. p19Arf-p53 tumor suppressor pathway regulates cell motility by suppression of phosphoinositide 3-kinase and Rac1 GTPase activities. J Biol Chem 2003;278:14414–9.
17. Guo F, Zheng Y. Rho family GTPases cooperate with p53 deletion to promote primary mouse embryonic fibroblast cell invasion. Oncogene 2004;23:5577–85.
18. Gadea G, de Toledo M, Anguille C, Roux P. Loss of p53 promotes RhoA-ROCK-dependent cell migration and invasion in 3D matrices. J Cell Biol 2007;178:23–30.
19. Sahai E. Mechanisms of cancer cell invasion. Curr Opin Genet Dev 2005;15:87–96.
20. Van Maerken T, Speleman F, Vermeulen J, et al. Small-molecule MDM2 antagonists as a new therapy concept for neuroblastoma. Cancer Res 2006;66:9646–55.
21. Secchiero P, Corallini F, Gonelli A, et al. Antiangiogenic activity of the MDM2 antagonist nutlin-3. Circ Res 2007;100:61–9.
22. Moskovits N, Kalinkovich A, Bar J, Lapidot T, Oren M. p53 Attenuates cancer cell migration and invasion through repression of SDF-1/CXCL12 expression in stromal fibroblasts. Cancer Res 2006;66:10671–6.
23. Dow L, Kauffman J, Caddy J, et al. The tumour-suppressor Scribble dictates cell polarity during directed epithelial migration: regulation of Rho GTPase recruitment to the leading edge. Oncogene 2007;26:2272–82.
24. Kuo J, Wang W, Yao C, Wu P, Chen R. The tumor suppressor DAPK inhibits cell motility by blocking the integrin-mediated polarity pathway. J Cell Biol 2006;172:619–31.
25. Gupta GP, Massague J. Cancer metastasis: building a framework. Cell 2006;127:679–95.
26. Pantel K, Brakenhoff RH. Dissecting the metastatic cascade. Nat Rev Cancer 2004;4:448–56.
27. Muller A, Homey B, Soto H, et al. Involvement of chemokine receptors in breast cancer metastasis. Nature 2001;410:50–6.
28. Taichman RS, Cooper C, Keller ET, Pienta KJ, Taichman NS, McCauley LK. Use of the stromal cell-derived factor-1/CXCR4 pathway in prostate cancer metastasis to bone. Cancer Res 2002;62:1832–7.
29. Koizumi K, Hojo S, Akashi T, Yasumoto K, Saiki I. Chemokine receptors in cancer metastasis and cancer cell-derived chemokines in host immune response. Cancer Sci 2007;98:1652–8.
30. Kedrin D, van Rheenen J, Hernandez L, Condeelis J, Segall J. Cell motility and cytoskeletal regulation in invasion and metastasis. J Mammary Gland Biol Neoplasia 2007;12:143–52.
31. Wyckoff J, Wang W, Lin EY, et al. A paracrine loop between tumor cells and macrophages is required for tumor cell migration in mammary tumors. Cancer Res 2004;64:7022–9.
32. Goswami S, Sahai E, Wyckoff JB, et al. Macrophages promote the invasion of breast carcinoma cells via a colony-stimulating factor-1/epidermal growth factor paracrine loop. Cancer Res 2005;65:5278–83.
33. Qian LW, Mizumoto K, Maehara N, et al. Co-cultivation of pancreatic cancer cells with orthotopic tumor-derived fibroblasts: fibroblasts stimulate tumor cell invasion via HGF secretion whereas cancer cells exert a minor regulative effect on fibroblasts HGF production. Cancer Lett 2003;190:105–12.
34. Murakami T, Maki W, Cardones AR, et al. Expression of CXC chemokine receptor-4 enhances the pulmonary metastatic potential of murine B16 melanoma cells. Cancer Res 2002;62:7328–34.
35. Sun YX, Schneider A, Jung Y, et al. Skeletal localization and neutralization of the SDF-1(CXCL12)/CXCR4 axis blocks prostate cancer metastasis and growth in osseous sites *in vivo*. J Bone Miner Res 2005;20:318–29.

AACR American Association for Cancer Research

Molecular Cancer Therapeutics

Nutlin-3a Induces Cytoskeletal Rearrangement and Inhibits the Migration and Invasion Capacity of p53 Wild-Type Cancer Cells

Diarmuid M. Moran and Carl G. Maki

Mol Cancer Ther 2010;9:895-905. Published OnlineFirst April 6, 2010.